PHYSICAL REVIEW B VOLUME 54, NUMBER 24 15 DECEMBER 1996-II

Hybridization of single- and double-layer behavior in a double-quantum-well structure

A. G. Davies, C. H. W. Barnes, K. R. Zolleis, J. T. Nicholls, M. Y. Simmons, and D. A. Ritchie
Cavendish Laboratory, Madingley Road, Cambridge CB3 0HE, United Kingdom
(Received 28 August 1996)

We report magnetoresistivity measurements of a narrow-barrier double-quantum-well structure which reveal that when two electron subbands are occupied, the positions of the diagonal resistivity maxima originating from these subbands oscillate together in magnetic field as the electron density is changed to give the overall appearance of a single-layer system. By means of Hartree calculations we demonstrate that this narrow-barrier sample is exhibiting a hybrid behavior between that of a single quantum well and a system comprising two independent quantum wells. [S0163-1829(96)50148-7]

Double-layer electron systems (DLES's) comprising two, high-quality, two-dimensional electron layers in close proximity are the natural extension to the single two-dimensional electron system (2DES) and a further step towards fully three dimensionally engineered quantum structures. They are formed in either a double-quantum-well structure where a large band-gap barrier separates the two electron sheets,[1] or a wide quantum well where the electron sheets are held apart by electrostatic repulsion.[2] DLES's have revealed a variety of new physical phenomena. For example, prominent single-particle integer quantum Hall states can be destroyed and replaced by many-body ground states,[1–3] and a new fractional quantum Hall state has been observed at filling factor $\nu=\frac{1}{2}$ (forbidden in single-layer systems).[4] Investigations of electron tunneling, electronic drag, and 2DES compressibility in DLES's have been equally fruitful.[5]

We identify a hybridization of single- and double-layer behavior in a narrow-barrier double quantum well by means of magnetoresistivity measurements and Hartree calculations. Although individual magnetoresistivity traces display manifestly double-layer behavior demonstrating that two electron subbands are occupied, the positions of the diagonal resistivity maxima originating from the two subbands oscillate together in magnetic field as the electron density is changed to give the overall appearance of a single-layer system.

Our DLES comprises two 150-Å-wide GaAs quantum wells separated by a 25-Å $Al_{0.33}Ga_{0.67}As$ barrier. A silicon-doped $Al_{0.33}Ga_{0.67}As$ layer is situated on either side of the double quantum well, offset by undoped $Al_{0.33}Ga_{0.67}As$ spacer layers. The DLES was processed into a Hall bar with a Schottky front gate and electrical contacts which connect both wells. The sample was mounted in a dilution refrigerator and magnetoresistivity measurements were performed using four-terminal, low-frequency ac techniques at 100 mK.

Figure 1(a) shows diagonal and Hall magnetoresistivity (ρ_{xx}, ρ_{xy}) traces for three gate biases (V_g). Insets I, II, and III show the corresponding calculated conduction-band edges and probability densities. The two lowest electron subbands E_1, E_2 ($E_1<E_2$), and the subband energy separation $\Delta(V_g)=E_2-E_1$ are identified in the schematic left inset (E_1 and E_2 both label the subbands and represent the subband energies). For $V_g=+0.10$ V (trace I, inset I), the wells are out of balance and the subband wave functions are predominantly confined within separate wells. As the system is progressively brought into balance (when the electron densities associated with each well are the same), the E_1 and E_2 wave functions are increasingly shared between the wells.[1,6] At the balance point ($V_g=-0.072$ V, trace II), E_1 and E_2 are the symmetric and antisymmetric eigenstates which extend equally across both wells and the subband separation is just the symmetric-antisymmetric gap ($\Delta=\Delta_{SAS}\approx 20$ K). At balance, the total density is $n=2.4\times10^{11}$ cm^{-2} and the mobility is 1.6×10^6 cm^2/V s in the dark. If V_g is decreased further, the front well depletes at $V_g\approx-0.49$ V and single-layer Shubnikov–de Haas (SdH) oscillations are observed from the back well (trace III). The electron densities associated

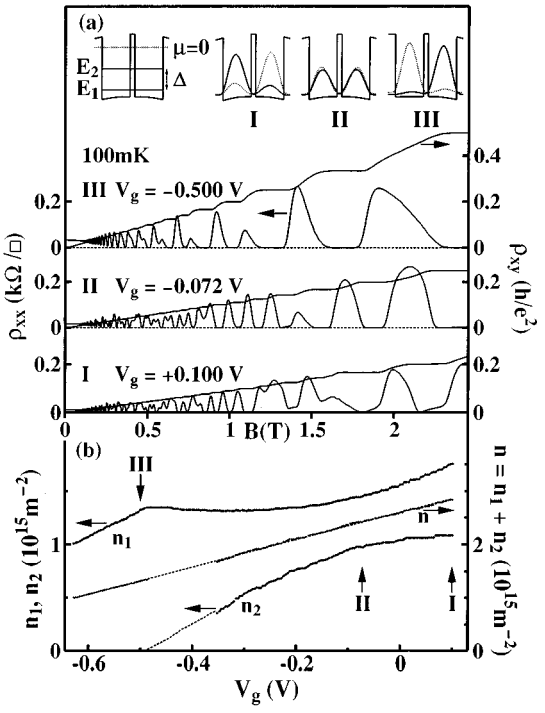

FIG. 1. (a) ρ_{xx} and ρ_{xy} vs B: (I) $V_g=+0.10$ V (off-balance), (II) $V_g=-0.072$ V (on-balance), (III) $V_g=-0.50$ V (front well depleted). Insets: Hartree conduction-band edges and probability densities. Schematic left inset defines E_1,E_2,Δ,μ. (b) Experimental n_1,n_2 vs V_g with total density $n=n_1+n_2$.

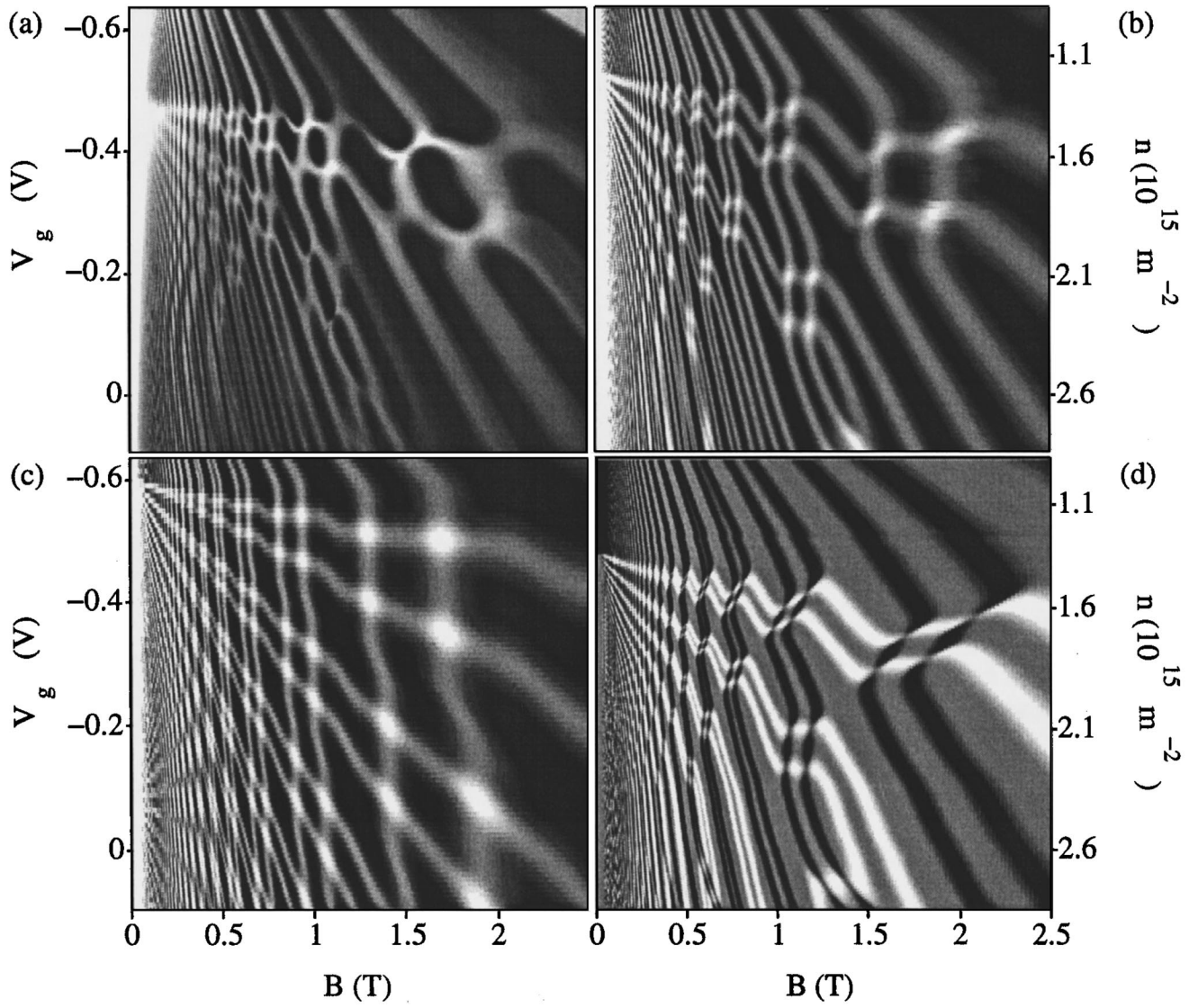

FIG. 2. $\rho_{xx}(B,V_g)$. (a) Experimental data, (b) Hartree calculation, and (c) localized wave-function calculation—white regions represent ρ_{xx} maxima. (d) Perfect subband locking calculation—black and white regions represent ρ_{xx} maxima originating from E_1 and E_2 subbands, respectively. In this figure ρ_{xx} is scaled by B for maximum contrast.

with the two subbands (n_1, n_2) obtained from the low-field SdH oscillations are shown as a function of V_g in Fig. 1(b) with the total electron density $n=n_1+n_2$ which varies linearly with V_g. The small increase in n_1 around $V_g \approx -0.47$ V has been attributed to exchange-induced charge transfer.[7]

Figure 2(a) shows ρ_{xx} as a function of perpendicular magnetic field (B) and V_g. White regions represent large ρ_{xx} (SdH oscillation maxima). For $V_g<-0.49$ V, the front well is depleted and the ρ_{xx} maxima trajectories of the back well map out the characteristic single-layer Landau level fan. As V_g is increased, the front well starts to populate and contribute to the conduction—the Landau fan from this subband emerges from the left axis at $V_g=-0.49$ V. For $V_g>-0.49$ V, it might be expected that the ρ_{xx} maxima of the front well would map out a single-layer Landau level fan while the positions of the ρ_{xx} maxima of the back well would be invariant in V_g, describing vertical lines in the figure, since the back well would be screened from the front gate. However, the contributions from the two subbands begin to oscillate and distort as B is increased, with the result that the trajectories of the single-layer Landau fan from the lower quantum well at the top of Fig. 2(a) are *preserved across the entire* $\rho_{xx}(B,V_g)$ *plot*, each trajectory defining a constant total filling factor $\nu=nh/eB$ $(\propto V_g h/eB)$.[8] The ρ_{xx} maxima trajectories associated with the two subbands oscillate in sympathy so that $\rho_{xx}(B,V_g)$ appears to derive from a single-layer system even though two subbands are occupied. This single-layer behavior is not that observed in the double- to single-subband occupancy transition investigated in single-quantum wells[8] and DLES's,[7] achieved by depopulation of one subband with a gate bias or via exchange interactions.[9] Circular features are formed in the $\rho_{xx}(B,V_g)$ plot by the intersection of the spin gaps of the two Landau ladders, but the distortion of the ρ_{xx} trajectories center these features where the Landau gaps in the E_1 subband [at $B=n_1(V_g)h/e2i$, with i an integer] coincide with the spin gaps in the E_2 subband [at $B=n_2(V_g)h/e(2j-1)$, with j an integer]. These circular

features appear to lie on a set of nested parabolas centered on the balance point.

We performed Hartree calculations[10,11] using appropriate functional forms for the Landau extended and total density of states.[12] Exchange and correlation effects were deliberately omitted. We calculate ρ_{xx} via the empirical relation $\rho_{xx} \approx B\Sigma_{i,\sigma}\wp_{i,\sigma}$, where $\wp_{i,\sigma}$ is the extended density of states at the chemical potential for spin σ and subband i. The calculated ρ_{xx} is presented in Fig. 2(b) and the striking comparison with Fig. 2(a) demonstrates that this calculation contains the essential physics behind the distortions in the trajectories of the ρ_{xx} maxima. This physics can be understood in terms of two limits: (i) the limit in which one subband wave function is localized in each well, and (ii) the limit in which both subband wave functions are delocalized across both wells. Limit (ii) applies to our DLES at the balance point.[1,6,13] Moving away from balance, the subband wave functions become progressively localized within the two wells and the DLES moves towards limit (i).

In limit (i) the DLES together with the front gate can be considered a triple-plate capacitor. If the distance between wells is large, then Landau levels from each subband appear independently at the chemical potential (μ) at fields determined by n_1 and n_2 and so the ρ_{xx} maxima mapped out as a function of V_g would follow $B_{\rho xx\ \max}(V_g) = n_{1,2}(V_g)h/e(i + \frac{1}{2})$, where i is an integer. However, the barrier width in our DLES is sufficiently small that the density-of-states contribution to the interlayer capacitance and the geometric contribution to the interlayer capacitance are comparable.[14] Consequently, as the thermodynamic density of states changes in magnetic field, the concomitant change in the interlayer capacitance causes charge to flow from one subband to the other (we discuss charge transfer in more detail below). The exact numerical solution for $\rho_{xx}(B,V_g)$ in the presence of disorder in this limit is shown in Fig. 2(c), calculated using the same Landau level and extended density of states as the Hartree calculation. The electron layers are taken to have zero thickness with separation equal to the well center-to-center distance (175 Å)—this gives the same interlayer geometric capacitance as measured experimentally. The front well starts to populate at $V_g \approx -0.6$ V in Fig. 2(c) because there is no tunneling gap in this limit. The trajectories of the ρ_{xx} maxima arising from the two subbands oscillate as a result of charge flow between subbands. This oscillation, however, is small in comparison with that observed in Fig. 2(a) and does not lead to the preservation of the single-layer Landau fan from the lower quantum well across the entire $\rho_{xx}(B,V_g)$ plot.

Now consider limit (ii). For the electron density to remain constant in a two-dimensional system as B is swept, the band edge (and subband energy) moves down in energy when a peak in the Landau level density of states is pinned at μ (the Fermi energy increases) and up in energy (the Fermi energy decreases) when μ is in a minimum of the Landau level density of states.[15] Since the subband wave functions are delocalized across the DLES in limit (ii) sharing the same confining potential, both subband energies are equally affected by the changing Landau level density of states at μ. Consequently, as B is swept, the subbands oscillate together, locked with fixed separation Δ. Because of this subband locking, the two Landau ladders effectively form a single ladder with only one level pinned at μ at any field (for zero disorder). Since all filled levels contribute eB/h to the total electron density irrespective of their origin, ρ_{xx} maxima occur when $n = (i + \frac{1}{2})eB/h$, where i is an integer and so in this limit $\rho_{xx}(B,V_g)$ is *identical* to that of a single layer. The exact numerical solution for $\rho_{xx}(B,V_g)$ in the presence of disorder assuming perfect subband locking is shown in Fig. 2(d), calculated using the same density of states as before and the experimental $n(V_g)$ and $\Delta(V_g)$. In Fig. 2(a) the ρ_{xx} maxima trajectories associated with the E_1 and E_2 subbands are displayed as black and white, respectively. The ρ_{xx} maxima trajectories distort in sympathy to give $\rho_{xx}(B,V_g)$ the appearance of a single layer with lines of constant total filling factor comprising alternating contributions from the two subbands. Consider an arbitrary ρ_{xx} maximum at $\nu = i + \frac{1}{2}$. When the front well is depleted, all occupied Landau levels are in E_1 in the back well so that $\nu_1 = i + \frac{1}{2}$ and $\nu_2 = 0$ (where ν_1 and ν_2 are the filling factors of the E_1 and E_2 subbands, respectively). As B and V_g are increased along the trajectory of constant ν, at some point the first Landau level in the E_2 subband will become occupied, $\nu_2 \rightarrow \frac{1}{2}$ and $\nu_1 \rightarrow i$. Each time ν_2 increases by $\frac{1}{2}$, ν_1 decreases by $\frac{1}{2}$ so this ρ_{xx} maximum derives alternately from the two subbands as observed. At the balance point this process is reversed and ultimately all occupied Landau levels will again be in E_1, but now in the front well.

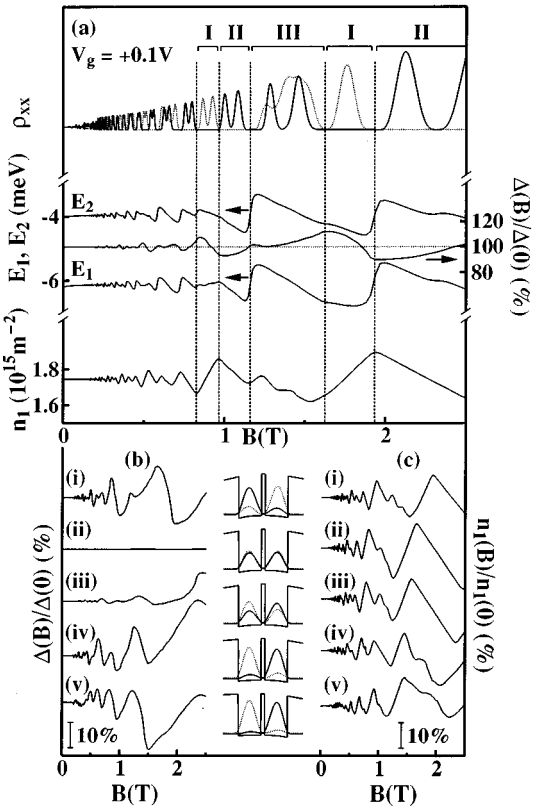

FIG. 3. (a) Hartree results for individual subband contributions to ρ_{xx} (E_1, solid trace; E_2, dashed trace), E_1, E_2, Δ, and n_1 at $V_g = +0.10$ V. (b),(c) Percent change in zero field value of Δ and n_1 vs B, respectively, for $V_g =$ (i) +0.10 V, (ii) balance, (iii) −0.11 V, (iv) −0.30 V, (v) −0.44 V. Insets: Hartree band edges and probability densities.

In general, a DLES will exhibit hybrid behavior between that of limits (i) and (ii). In order to demonstrate how this hybridization occurs, we discuss the detailed electrostatics of our DLES at an arbitrary gate bias. Figure 3(a) shows E_1, E_2, Δ, n_1, and the individual subband contributions to the total ρ_{xx} obtained from our Hartree calculations, for $V_g=+0.10$ V. Consider Δ and n_1 in regions I and II. In region I, a spin-split Landau level in the E_2 subband is pinned at μ and the highest occupied Landau level in the E_1 subband lies below μ (ρ_{xx} maxima in this region derive from E_2). As B increases, Δ decreases accompanied by an increase in n_1. In region II, a spin-split Landau level in the E_1 subband is pinned (ρ_{xx} maxima derive from E_1), and as B increases, Δ increases and n_1 decreases. (The behavior in region III is complicated by the crossing of Landau levels at μ.) Charge transfers out of the subband which has a Landau level pinned at μ into the other subband, keeping n invariant to within small capacitive corrections. Figures 3(b) and 3(c) show the calculated Δ and n_1 as a function of B for a series of V_g, together with corresponding band-edge profiles and probability densities. Moving away from balance, the wave functions become progressively localized in the wells and there is a reduction in charge transfer [$n_1(B)$ oscillates less] and a weakening of subband locking [$\Delta(B)$ oscillates more]. The charge transfer moderates the relative motion of the two subbands and produces a tendency for them to lock together. Since the subband wave functions occupy the same physical space in limit (ii), there is no capacitive energy cost for the transfer of charge between subbands, and so $n_1(B)$ oscillates maximally. In limit (i) there is a capacitive energy cost to transfer charge between subbands since the subband wave functions are spatially separated, therefore $\Delta(B)$ oscillates maximally in this limit and the transfer of charge is restricted. In general, the ρ_{xx} maxima continuously move from the positions shown close to the balance point in Fig. 2(d) towards those shown away from balance in Fig. 2(c) as a result of the changes in subband locking and charge transfer. In our device we never access true limit (i) behavior. There is sufficient wave-function delocalization between the two wells in our narrow-barrier DLES for limit (ii) single-layer behavior to be predominant over the entire V_g range, although away from balance, some aspects of the $\rho_{xx}(B,V_g)$ plot (e.g., the shape of the circular features) are better represented by the localized wave-function calculation [limit (i)] demonstrating that the system behaves as a hybrid of these limits.

In conclusion, we have observed a distortion in the positions of the ρ_{xx} maxima in a narrow-barrier DLES which gives the overall appearance of a single-layer system. We explain this phenomenon in terms of wave-function delocalization, subband locking, and charge transfer between subbands. These effects will be generic to any electronic system in which two discrete densities of states are brought into contact—e.g., coupled 1D systems or quantum antidots (around which a series of bound states condense out of each Landau level at high field).

A.G.D. and C.H.W.B. thank the Royal Society and the Isaac Newton Trust. K.R.Z. and D.A.R. acknowledge TCRC. We thank F. Stern and C. J. B. Ford for discussions. This work was funded by the EPSRC (UK).

[1] G. S. Boebinger *et al.*, Phys. Rev. Lett. **64**, 1793 (1990).
[2] Y. W. Suen *et al.*, Phys. Rev. B **44**, 5947 (1991).
[3] G. S. Boebinger *et al.*, Phys. Rev. B **45**, 11 391 (1992); S. Q. Murphy *et al.*, Phys. Rev. Lett. **72**, 728 (1994); A. H. MacDonald *et al.*, *ibid.* **65**, 775 (1990).
[4] Y. W. Suen *et al.*, Phys. Rev. Lett. **68**, 1379 (1992); J. P. Eisenstein *et al.*, *ibid.* **68**, 1383 (1992).
[5] J. P. Eisenstein, in *High Magnetic Fields in Semiconductor Physics*, edited by D. Heiman (World Scientific, Singapore, 1995), p. 78 and references therein.
[6] A. Palevski *et al.*, Phys. Rev. Lett. **65**, 1929 (1990).
[7] X. Ying *et al.*, Phys. Rev. B **52**, R11 611 (1995); Y. Katayama *et al.*, *ibid.* **52**, 14 817 (1995); N. K. Patel *et al.*, *ibid.* **53**, 15 443 (1996).
[8] I. S. Millard *et al.*, J. Phys. Condens. Matter **8**, L311 (1993).
[9] A. R. Hamilton *et al.*, Phys. Rev. B **51**, 17 600 (1995).
[10] P. P. Ruden *et al.*, Appl. Phys. Lett. **59**, 2165 (1991).
[11] A. Kumar *et al.*, Phys. Rev. B **42**, 5166 (1990).
[12] Parameters taken from *Properties of Aluminium Gallium Arsenide*, edited by S. Adachi (INSPEC, London, 1993). Total and extended density of state widths of 0.055 and 0.018 meV were chosen by fitting one experimental SdH trace at $V_g=-0.6$ V. A constant effective g factor ($g^*=-3$) was used for simplicity—it is an overestimate at low B and an underestimate at high B.
[13] C. H. W. Barnes *et al.*, Surf. Sci. **361/362**, 608 (1996).
[14] In some DLES's many-body effects remove this delocalization; see Refs. 1–3.
[15] S. Luryi, Appl. Phys. Lett. **52**, 501 (1988); J. P. Eisenstein *et al.*, Phys. Rev. B **50**, 1760 (1994).
[16] T. Ando *et al.*, Rev. Mod. Phys. **54**, 437 (1982); V. M. Pudalov *et al.*, Zh. Eksp. Teor. Fiz. **89**, 1870 (1985) [Sov. Phys. JETP **62**, 1079 (1985)]; D. G. Hayes *et al.*, Phys. Rev. B **44**, 3436 (1991).